Atomic vapor deposition of bismuth titanate thin films

Nitin Deepak, Panfeng F. Zhang, Lynette Keeney, Martyn E. Pemble, and Roger W. Whatmore

Citation: J. Appl. Phys. **113**, 187207 (2013); doi: 10.1063/1.4801985
View online: http://dx.doi.org/10.1063/1.4801985
View Table of Contents: http://jap.aip.org/resource/1/JAPIAU/v113/i18
Published by the American Institute of Physics.

JOURNAL OF APPLIED PHYSICS **113**, 187207 (2013)

Atomic vapor deposition of bismuth titanate thin films

Nitin Deepak,[a] Panfeng F. Zhang, Lynette Keeney, Martyn E. Pemble, and Roger W. Whatmore
Tyndall National Institute, University College Cork, 'Lee Maltings', Dyke Parade, Cork, Ireland

(Received 1 October 2012; accepted 6 March 2013; published online 8 May 2013)

c-axis oriented ferroelectric bismuth titanate ($Bi_4Ti_3O_{12}$) thin films were grown on (001) strontium titanate ($SrTiO_3$) substrates by an atomic vapor deposition technique. The ferroelectric properties of the thin films are greatly affected by the presence of various kinds of defects. Detailed x-ray diffraction data and transmission electron microscopy analysis demonstrated the presence of out-of-phase boundaries (OPBs). It is found that the OPB density changes appreciably with the amount of titanium injected during growth of the thin films. Piezo-responses of the thin films were measured by piezo-force microscopy. It is found that the in-plane piezoresponse is stronger than the out-of-plane response, due to the strong *c*-axis orientation of the films. © *2013 AIP Publishing LLC* [http://dx.doi.org/10.1063/1.4801985]

I. INTRODUCTION

Ferroelectrics are a valuable class of functional materials due to their polar switchability and strong piezoelectric, pyroelectric effects, etc. These properties can be used for various applications, e.g., ferroelectric random access memories (FeRAM),[1] actuators,[2] etc. Good quality epitaxial ferroelectric thin films are highly desirable for integrated memories and MEMS applications for which they show better properties than randomly oriented polycrystalline films.

The Aurivillius phase[3] ferroelectrics, with general formula $[(Bi_2O_2)\ (A_{n-1}B_nO_{3n+1})]$, are layer structured materials consisting of "n" perovskite layers formula $(A_{n-1}B_nO_{3n+1})^{2-}$ interleaved between two bismuth oxide $(Bi_2O_2)^{2+}$ layers. These materials possess interesting ferroelectric and piezoelectric properties, which can be tailored by altering the value of "n" and substituting various types of ions in the perovskite layers. $Bi_4Ti_3O_{12}$ (BTO) is a member of Aurivillius family with n = 3 and when doped with, e.g., La and Nd, it is a good candidate for non-volatile ferroelectric memory devices due to its excellent fatigue-free performance.[4] The electric polarization direction in BTO is in the *a*-*c* plane,[5] with major polarization axis ($50\ \mu C\,cm^{-2}$) along the "*a*" direction and minor polarization axis ($4\ \mu C\,cm^{-2}$) along the "*c*" direction. The ferroelectric properties of these materials in thin film form are greatly influenced by the presence of defects, such as point defects, lines defects, oxygen vacancies, and out-of-phase boundaries (OPBs). For example, oxygen vacancies[6] cause large leakage currents by providing leakage paths. In the present study, epitaxial BTO thin films were prepared using an Aixtron atomic vapor deposition (AVD)[7] system in a layer-by-layer growth mode. The presence of OPBs was detected by x-ray diffraction (XRD) and transmission electron microscopy. The effect of changing experimental conditions on the occurrence of OPBs and their formation mechanism are discussed.

Piezo-force microscopy (PFM)[8] is a powerful tool to analyze the nano scale piezo-response, which makes it useful for probing the piezoelectric domain structures of thin films, nano-structures, and even biological materials.[9] An AC voltage is applied through a nano sized conducting tip, in contact with the sample surface. The sample will contract or expand locally in the direction of an applied electric field, due to the converse piezo-electric effect. This contraction or expansion in the sample deflects the cantilever in-phase or out-of-phase with the applied electric field. In this way, ferroelectric domains can be probed at nano-scale. This method is very sensitive, with resolution up to a few pico-meters in the z-direction.

II. EXPERIMENTAL SECTION

A. Growth of $Bi_4Ti_3O_{12}$ thin films

BTO thin films were grown using the Aixtron AIX 200 4/FE AVD system. In this system, liquid precursors are injected (either sequentially or as a mixture) into a vaporizer in which they are instantly vaporized, the vapors then being carried over a heated substrate using N_2 carrier gas. The precursors used for growth were $Bi(thd)_3$ (thd = 2,2,6,6-tetramethyl-3,5-heptanedionate) and $Ti(O\text{-}iPr)_2(thd)_2$ (where O-iPr = iso-propoxide) as 0.1 M solutions in toluene. Computer control allows micro-liter volumes of precursor solution to be injected into vaporizer, which was kept at 220 °C, with the vapors being carried to the growth chamber through lines also kept at 220 °C. The growth chamber was a typical cold wall reactor with a susceptor heated substrate holder held at 650 °C in this work. There are previous reports of BTO thin films grown by metal organic chemical vapor deposition (MOCVD),[10,11] but at temperatures higher than 650 °C. (001) oriented $SrTiO_3$ (STO) single crystal substrates were cleaned with acetone and iso-propanol prior to growth. The substrates were rotated with 60 sccm nitrogen flow through a susceptor holder to obtain improved uniformity. The pressure of the growth chamber was kept at 10 mbar. Pure oxygen was used as an oxidizing agent. The total gas flow in the growth chamber was 3000 sccm in which the oxygen flow was 1000 sccm. The amount of bismuth and titanium precursor was controlled by changing the opening time

[a]nitin.deepak@tyndall.ie.

of computer controlled injectors and by altering the number of pulses as discussed below. The amount of precursor injected was monitored with a liquid flow meter. The precursor flow can be easily controlled to insert a monolayer of TiO_2. The growth of BTO thin films was accomplished using the sequenced mode shown in Figure 1. The sequence is the same as the structure of BTO along the c-axis with the blue-colored bar representing one bismuth set. This set consists of different numbers of pulses with different injector opening time (usually several 10^{-3} s) to change the amount of bismuth precursor injected. The pulse injection frequency was 1 Hz. The time gap between one set of pulses was kept constant at 5 s. The size of each pulse set was changed with the number of pulses and opening time and same was the case with titanium set, shown in red. The total set shown in Figure 1 represents one loop, equivalent to one half of a BTO unit cell. This was repeated 20 times to get approximately 33 nm thickness, which is the thickness of 10 unit cells of BTO. This type of sequenced mode was used before to prepare BTO thin films on Pt/Si substrates by MOCVD.[12] The present study reports the use of this sequence with a liquid injection system on STO substrates for the first time. To study the effect of precursor injection on the growth of bismuth titanate thin films, the amount of bismuth precursor is varied, while keeping the injection of titanium constant and vice versa.

B. Characterization of thin films

The crystalline structure of the films was examined using a Philips PANalytical MRD XRD system with Cu-Kα radiation at room temperature. A MFP-3D^{TM} (Asylum Research) atomic force microscope (AFM) was used in contact mode for topography mapping of the films. Olympus AC160TS silicon probes were used for imaging with AFM. A Jeol 2100 transmission electron microscope (TEM) with a double tilt holder was used for high resolution transmission electron images at 200 kV voltages. TEM samples were prepared using focused ion beam thinning procedures. Electromechanical responses of the films were measured by PFM using an Asylum Research MFP-3D^{TM} PFM system in contact mode equipped with a high voltage amplifier. Single frequency PFM was used to image in-plane piezo-response. In-plane electromechanical responses were imaged using the single frequency lateral PFM mode with driving frequency lower than contact resonance to avoid the cross-talking. Out-of-plane piezo-response of the films were investigated by Single Frequency and Dual AC Resonance Tracking PFM (DART-PFM)[13] modes. Olympus AC240TM PFM silicon cantilevers coated with Ti/Pt with contact resonance frequency around 320 kHz were used for PFM imaging.

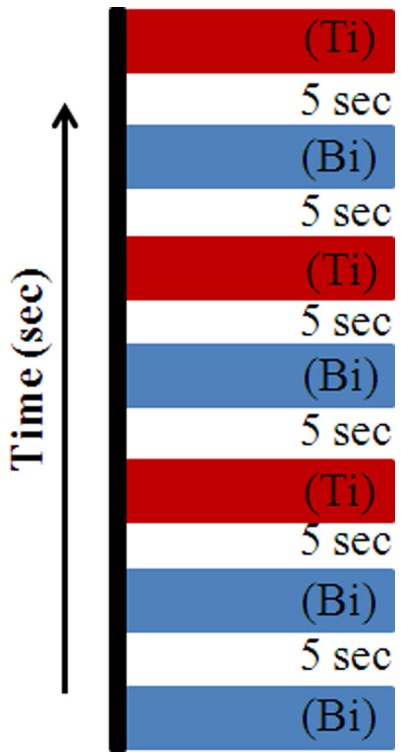

FIG. 1. The growth mode used for bismuth titanate thin film growth.

III. RESULTS AND DISCUSSION

A. Thin film crystalline properties

Two different experiment sets were performed. In the first set, the amount of titanium precursor was kept constant while varying the amount of bismuth precursor, to observe the effect of bismuth injection on the crystalline properties. In the second set, the amount of bismuth precursor was kept constant while varying the amount of titanium precursor.

In the first set of experiments, the Bi:Ti ratio was varied between 2.50 to 6.30. The XRD data presented in Figure 2 show that the films were highly *c*-axis oriented, with no impurity phases observed. Peaks indicated with an asterisk (*) are from the substrate and sample holder. The legends on the XRD data show the volumetric Bi:Ti ratio, and the data are plotted in log scale to make weak peaks visible. A manual offset was used to make different data sets visible on one graph. A higher amount of bismuth than the stoichiometric ratio was used to compensate for bismuth loss[14] in the film during growth due to the volatile nature of bismuth and the low deposition efficiency of the bismuth precursor.[15] Excess

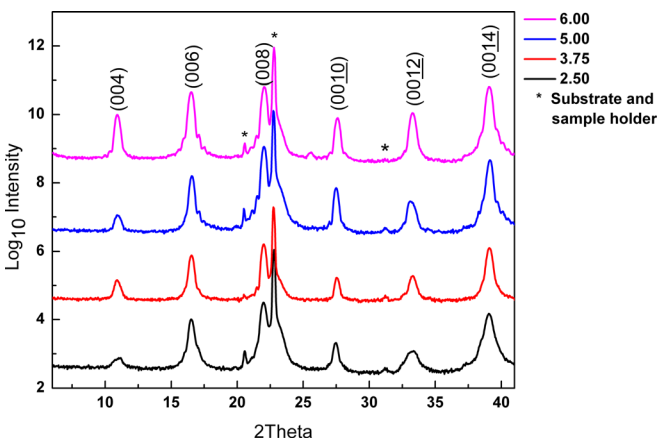

FIG. 2. The effect of bismuth precursor injection on the crystalline properties of bismuth titanate thin films. The legend indicate Bi:Ti volumetric ratio.

bismuth was previously used to grow $Bi_4Ti_3O_{12}$ with molecular beam epitaxy (MBE) by Theis *et al.*,[16] to achieve adsorption controlled growth. Similar kinds of adsorption-controlled growth were used by Keijser *et al.* for $Pb(Zr,Ti)O_3$ thin films grown by MOCVD.[17] From Figure 2, the effect of bismuth precursor volume can be clearly seen. The peaks become sharper as the Bi:Ti ratio was increased. This effect is most prominent in the (004) and (00$\underline{12}$) peaks. The full width half maxima (FWHM) decreased from 0.6714 to 0.3366 for (004) peak when the amount of bismuth increased (Bi:Ti ratio changed from 2.5 to 6.0). FWHM reached its minimum of 0.3366 at Bi:Ti ratio of 6.0.

In order to compare the relative crystallinity of various samples, a relative crystalline quality parameter Q is defined as $1/(BCos\,\theta)$, where "B" is the peak breadth (FWHM) in radians and "θ" is incident x-ray beam angle. (This was derived from the Scherrer formula[18] ($t = 0.9\lambda/(BCos\,\theta)$, is crystal size and "$\lambda$" is the wavelength of the x-ray beam). In Figure 3, $Q = 1/(BCos\,\theta)$ was averaged over (004), (006), (00$\underline{10}$), (00$\underline{12}$), and (00$\underline{14}$) peaks, was plotted against Bi:Ti ratio. It can be seen that the crystalline quality increased with increase in the Bi:Ti ratio and reached its maximum at Bi:Ti ratio 6.0.

A second experiment was conducted with the amount of bismuth precursor set and kept constant at a value that gave the lowest FWHM in the first set of experiments, and then the amount of titanium precursor was changed so that the Bi:Ti ratio was varied between 3.80 and 7.60. In Figure 4, the effect of titanium injection per set of pulses can be clearly seen. The amount of titanium per pulse set (one titanium set) has a great effect on the crystalline properties of the film; as the amount of titanium in one set of pulses was increased (meaning that Bi:Ti ratio was decreased), the crystallinity improved, which can be inferred from the lowering of the FWHM of the (004) peak. The FWHM minimised at a at value 0.3362° for a Bi:Ti ratio of 6.0. As the amount of titanium is increased further, with Bi:Ti ratio at 5.60, the FWHM increases to 0.3839° and finally as Bi:Ti ratio reaches 5.40, a splitting of the (004) and (00$\underline{12}$) peaks occurs. The splitting persisted on decreasing Bi:Ti ratio finally disappearing at a Bi:Ti ratio of 3.0.

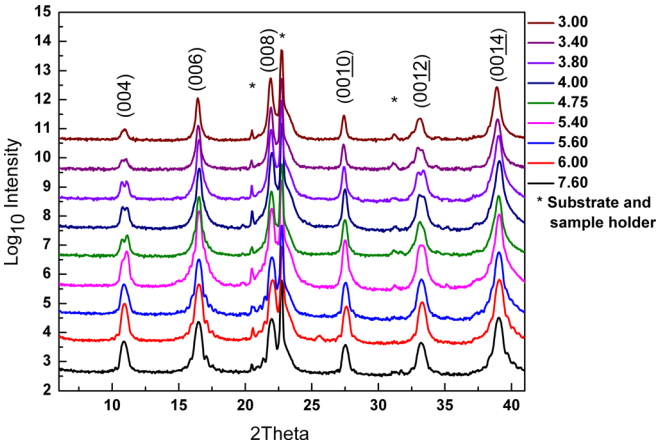

FIG. 4. The effect of titanium precursor injection on crystalline properties of bismuth titanate thin film. The legend indicates Bi:Ti volumetric ratio.

At first sight, this splitting might be considered as pointing towards the existence of a BTO phase with a slightly different *c*-axis or perhaps to the existence of some other phase. However, it is more likely to be caused by OPB defects. OPBs were previously observed in MBE growth of BTO by Pan *et al.*[19] and are common in epitaxial films of Aurivillius compounds.[20] For example, the epitaxial $SrTa_2Bi_2O_9$ (SBT) system also shows OPBs.[20] An OPB is a boundary between two parts of crystal relatively displaced with respect to one another, such that the magnitude of displacement parallel to the z-direction is "c/x"[20] ("c" is the lattice parameter). Under condition x = 2, the OPBs are called anti-phase boundaries where displacement is exactly half of c. These defects frequently occur[20] in layer-by-layer growth mode. This is because in this kind of growth modes, slight change in stoichiometry causes change in local crystal structure, which in turn gives rise to these defects. TEM analysis was used to confirm the presence of OPBs. The cross-sectional TEM images in Figure 5 confirm the presence of OPBs. The displacement that occurs between two adjacent layers of BTO at OPBs is calculated from TEM data, and its magnitude is approximately 0.4 nm (within experimental error). This value is very close to the height of the steps on STO substrates.

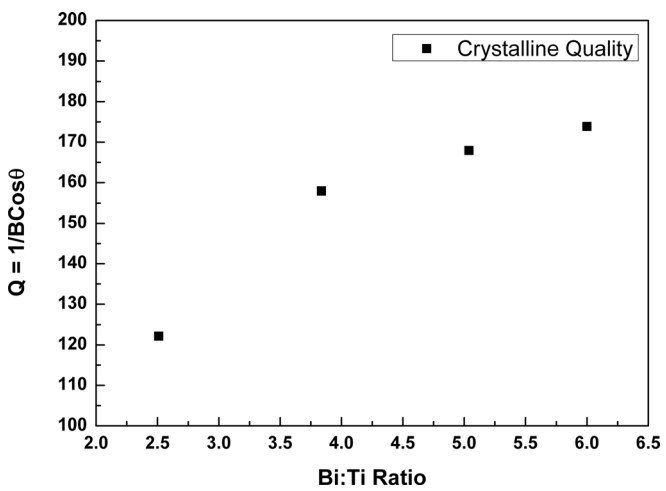

FIG. 3. The relative crystalline quality 1/(BCos θ) plotted against Bi:Ti ratio for (008) peak for the first set of experiments Here, B is peak broadening and θ is the incident x-ray beam angle in radians.

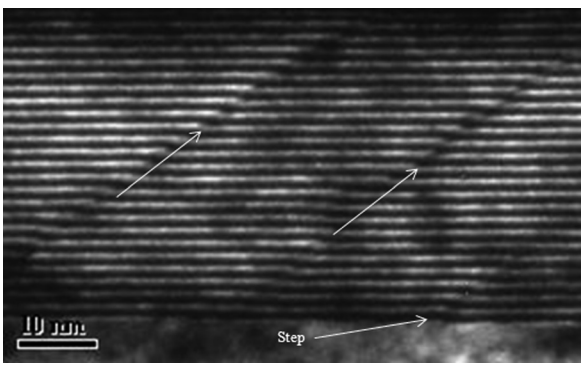

FIG. 5. High resolution TEM images of OPB's in bismuth titanate thin films and steps on STO substrates.

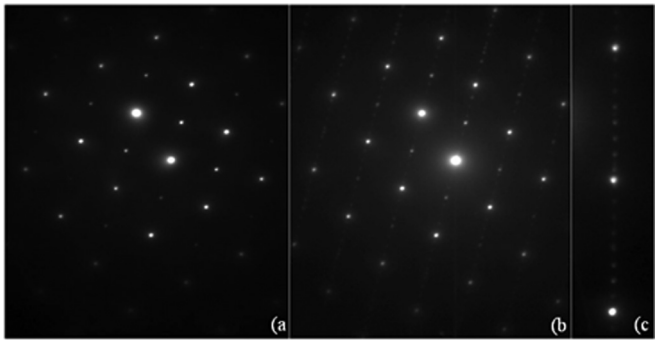

FIG. 6. The SAED pattern for (a) STO substrate, (b) STO+BTO, and (c) BTO super-lattice.

Figure 6 confirms the epitaxial nature of BTO thin films. In this figure, the selected area electron diffraction (SAED) pattern for the STO substrate, the STO substrate with the BTO thin film, and the BTO superlattice are shown. The BTO[100] direction is parallel to STO[110] direction. BTO film grows at 45° offset from [100] direction of STO to achieve this epitaxial relation.

A similar kind of splitting was observed by Zurbuchen *et al*. in SBT.[20] There, a peak splitting was observed in the (008), (0014), and (0020) peaks, but in the BTO system, only the ($00\overline{4}$) and ($00\overline{12}$) peaks show splitting. Zurbuchen *et al*.[20] proposed that in SBT, the XRD peak splitting gives a qualitative measure of the density of OPBs, a large peak splitting meaning a high OPB density and vice-versa. The same kind of splitting pattern was observed in our XRD data for the BTO thin films. Large peak splitting of the (004) and ($00\overline{12}$) peaks, observed in the films, demonstrating higher OPB densities, which were confirmed by TEM. The change in OPB density and its effect upon peak splitting can be clearly seen in the TEM images in Figure 7, where samples with higher splitting in the XRD peaks demonstrate a higher volume of OPBs. The cross-sectional TEM image for the sample with Bi:Ti ratio 4.75 is shown in Figure 7(a). Figure 7(b) shows TEM cross-sectional images for samples with Bi to Ti ratio of 3.4 with the corresponding (004) XRD data in Figure 7(c) for comparison. It is clear from the TEM images that the higher peak splitting in the XRD data is symptomatic of a higher OPB density.

In order to understand the behavior of crystalline quality in BTO thin films system $Q = 1/(BCos\,\theta)$ was plotted against

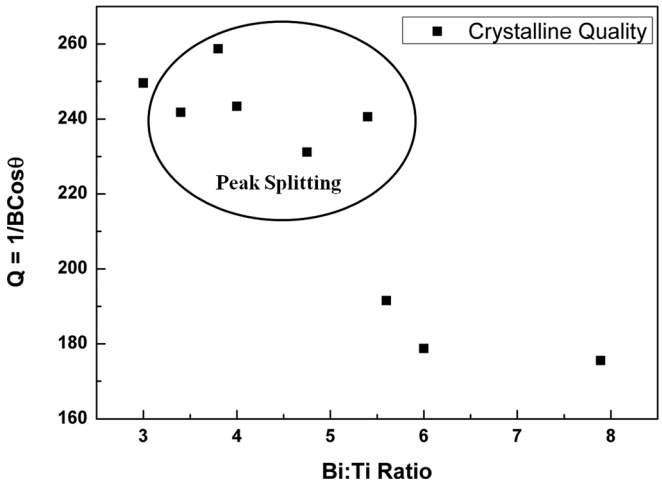

FIG. 8. The relative crystalline quality 1/(BCos θ) plotted against Bi:Ti ratio for (008) peak for the second set of experiments. Points inside the circle are samples with OPBs. Here, B is peak broadening and θ is the incident.

Bi:Ti ratio for the second set of samples. The data were averaged over the (006), (00$\underline{10}$), and (00$\underline{14}$) peaks and is presented in Figure 8 (The (004) and (00$\underline{12}$) peaks were excluded due to presence of splitting). An interesting trend was observed from this plot. As the Bi:Ti ratio decreased below 5.60, i.e., in the region where OPBs start to occur, a jump in crystalline quality was observed. This means that the samples containing OPBs have better overall crystalline quality as measured by peak FWHM when compared with the samples without OPBs. The reason for improved crystalline quality of the films with OPB defects in BTO system is that the atomic arrangement changes in such a way that it gives rise to a better crystalline structure, hence the increased quality factor.

Different reasons were discussed in order to explain the origin of these OPBs.[20] One of the reasons for the OPBs to occur can be the atomic steps on the STO substrate surface, as these steps act as nucleation sites for OPBs. The origination of OPBs at substrate can be clearly seen in Figure 5. Another reason could be a change in local stoichiometry, which causes these OPBs to occur.

In the present case of the growth of BTO by AVD, as the Bi:Ti ratio decreased (or amount of titanium increased) from 5.60, the splitting in the XRD peaks started to appear. This splitting disappears when Bi:Ti ratio reaches 3.00 (Figure 3). At Bi:Ti ratio = 6.00, where the FWHM was a

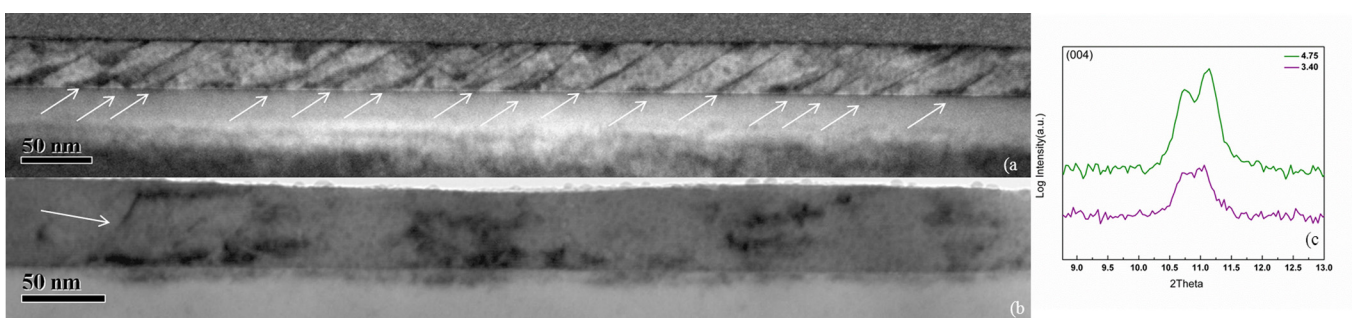

FIG. 7. Representative TEM images of BTO samples with (a) large (Bi:Ti ratio 4.75) and (b) small (Bi:Ti ratio 3.40) (c) corresponding XRD data showing extent of 2Theta splitting splitting for the 004 reflection from each sample.

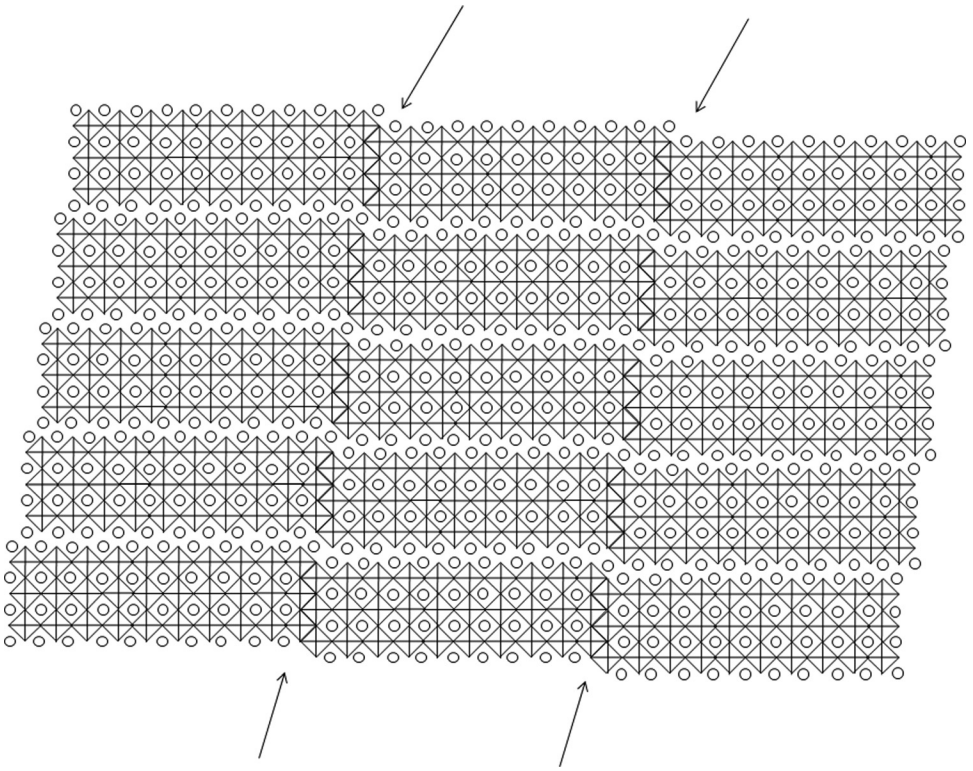

FIG. 9. Representative image of structural changes that may occur due to incorporation of OPBs. Circles represent position of bismuth atoms and titanium atoms are at center of octahedrons. Oxygen atoms are not shown here. (Reproduced with permission from Zurbuchen *et al.*, "Morphology, structure, and nucleation of OPBs in epitaxial films of layered oxides," J. Mater. Res. **22**(6), 1439 (2007). Copyright 2007 Cambridge University Press.)

minimum for (004), the growth rate was approximately one monolayer of TiO_2 per set of titanium precursor. When Bi:Ti ratio decreased from 6.00 and the amount of titanium becomes more than one monolayer per titanium set, the splitting start to appear. It seems, therefore, that an off-stoichiometry due to increased titanium in the system leads to these OPBs. When the amount of titanium per set of pulses gets doubled (Bi:Ti ratio 3.00), the splitting in the peaks disappears. In this case, the injection of titanium per set of pulses, increased from monolayer to bi-layer and splitting disappears.

Considering the possibility of bismuth loss could be responsible for the OPBs in the system, due to the volatile nature of bismuth; this may change local stoichiometry and in turn, change in crystalline structure, hence giving rise to splitting in peaks. However, in the first set of experiments where the amount of titanium was kept constant, no splitting was observed in any peaks, even at very low bismuth conditions. This evidence points towards the splitting, being related more to titanium injection than bismuth injection. If the amount of titanium in the films is more than required by stoichiometry, crystal structure changes may occur to accommodate this extra amount of titanium. Figure 9 shows the possible structure that might form due to higher amount of titanium. In this figure, arrows are pointed towards the region where these structural changes occur. The TiO_6 octahedra change from corner sharing to edge sharing, effectively removing Bi from the lattice locally, and decreasing the Bi:Ti ratio. Hence, the insertion of OPBs into the lattice allows it to accommodate more Ti, and the higher the concentration of OPBs, the lower the Bi:Ti ratio. Detailed theoretical work is in progress to quantitatively relate OPB density to composition and XRD peak splitting to explain why only (004) and (00$\underline{12}$) peaks split and why the introduction of a Ti bi-layer at $\overline{\text{Bi}}$:Ti = 3.0 eliminates the OPBs, an observation which is not currently understood.

B. Thin film morphology and piezo-force microscopy analysis

The surface of BTO thin films was characterized with AFM in contact mode. AFM height image is shown in Figure 10. The films are relatively smooth, and the RMS roughness is 1.4 nm. Single frequency PFM was used to probe the domain structure in-plane and out-of-plane. For this purpose, 60 nm BTO thin films are grown on Nb-doped STO substrates with Bi:Ti ratio 5.2 were analyzed. Figure 11 shows the difference between in-plane and out-of-plane piezo-response as a result of applying AC voltage with a

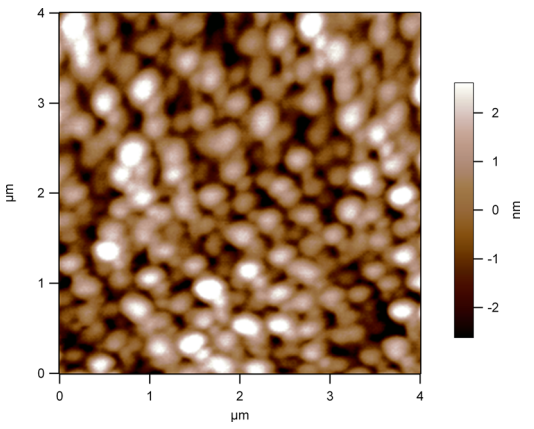

FIG. 10. Representative AFM height image for 4 μm × 4 μm areas of BTO thin film (Bi:Ti ratio 5.20).

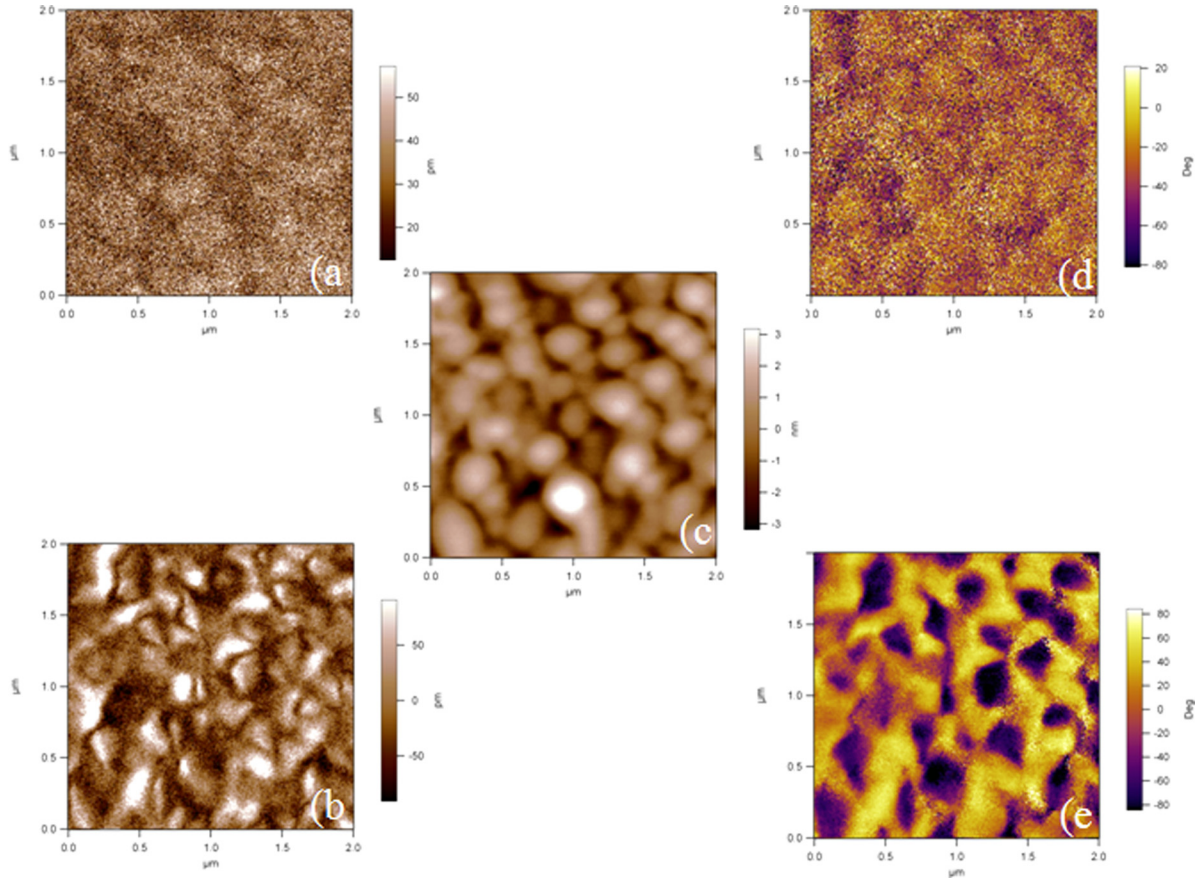

FIG. 11. Representative single frequency (a) out-of-plane PFM amplitude, (b) in-plane PFM amplitude, (c) height, (d) out-of-plane PFM phase, and (e) in-plane PFM phase in 2 μm $\times$ 2 μm areas of BTO thin film (Bi:Ti ratio 5.20).

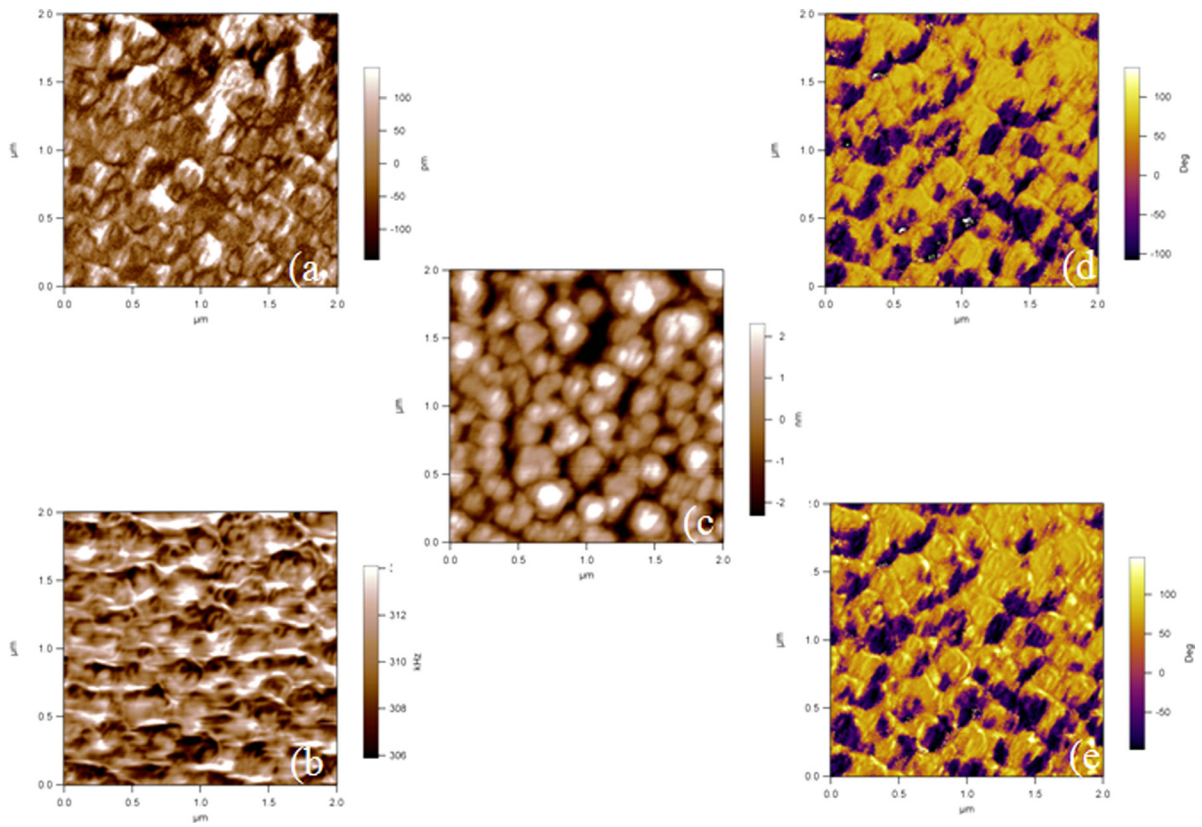

FIG. 12. Representative DFRT (a) PFM amplitude, (b) PFM frequency, (c) Height, (d) PFM phase one, and (e) PFM phase two in 2 μm $\times$ 2 μm areas of BTO thin film (Bi:Ti ratio 5.20).

conducting PFM tip. The frequency for in-plane measurements was kept lower than contact resonance to avoid cross-talk. In-plane piezo-response is much stronger than out-of-plane piezo-response due to the anisotropy of electric polarization, which is expected as films are epitaxial. Figures 11(a) and 11(b) demonstrates the difference between in-plane and out-of-plane amplitudes and Figures 11(d) and 11(e) shows the difference between in-plane and out-of-plane phases, corresponding to height image shown in Figure 11(c). In-plane domain structure can be clearly seen in the phase image in Figure 11(b); different domain orientation can be observed in the different colors. Yellow and purple colors show domain with opposite orientation. DART[13] PFM mode was used to investigate out-of plane piezo-response. Since piezo-response out-of-the plane is very small, the DART mode enables PFM imaging out-of-plane by using the sample-cantilever contact resonance to enhance the signal, while minimizing the effects of topography cross-talk. Figure 12 shows the resonance enhanced out-of plane PFM images. Figure 12(a) shows DART phase image, Fig. 12(b) shows frequency, Figure 12(d) shows phase one, and Figure 12(e) shows phase two corresponding to height image shown in Figure 12(c). Domains with different orientations can be seen clearly in these figures.

IV. CONCLUSIONS

Bismuth titanate thin films were successfully grown on (001) $SrTiO_3$ substrates. The sequenced growth mode was used with an AVD system to fabricate epitaxial films with greater control over processing conditions and at temperatures as low as 650 °C without the need for any post-deposition annealing. The films are smooth with RMS roughness of 1.4 nm. This work demonstrates how off-stoichiometry in the films affects their crystal structures and causes OPB defects. (004) and (00$\overline{12}$) peak splits give information about the OPB density in BT$\overline{O}$ thin film system; however, it is still not clear why the splitting occurs in these two peaks only. PFM experiments have shown that the BTO thin films have large in-plane piezo-response as compared to out-of plane piezo-response, as would be expected from such strongly c-axis orientated films.

ACKNOWLEDGMENTS

We are thankful to Dr. Simon Newcomb (Glebe Scientific) for TEM analysis. The authors acknowledge ICGEE (International Centre for Graduate Education in micro and nano Engineering) for funding Nitin Deepak's Ph.D. The support of Science Foundation Ireland (SFI) under the FORME Strategic Research Cluster Award No. 07/SRC/I1172 was greatly acknowledged. This research was also enabled by the Higher Education Authority Program for Research in Third Level Institutions (2007-2011) via the INSPIRE program.

[1]J. F. Scott and C. A. P. D. Araujo, Science **246**(4936), 1400–1405 (1989).
[2]P. Muralt, J. Micromech. Microeng. **10**, 136–146 (2000).
[3]B. Aurivillius, Ark. Kemi. **1**, 499 (1950).
[4]J. Arreguín-Zavalaa, M. E. Villafuerte-Castrejóna, F. Gonzáleza, L. Buciob, O. Novelo-Peraltaa, R. Y. Sato-Berrúc, and J. Ocotlán-Floresc, Mater. Character. **60**(3), 219–224 (2009).
[5]S. E. Cummins and L. E. Cross, J. Appl. Phys. **39**, 2268–2275 (1968).
[6]J. F. Scott and M. Dawber, Appl. Phys. Lett. **76**, 3801–3803 (2000).
[7]U. Weber, M. Schumacher, J. Lindner, O. Boissiere, P. Lehnen, S. Miedl, P. K. Baumann, G. Barbar, C. Lohe, and T. McEntee, Microelectr. Reliab. **45**, 945–948 (2005).
[8]A. Gruverman, O. Auciello, and H. Tokumoto, Annu. Rev. Mater. Sci. **28**, 101–123 (1998).
[9]S. V. Kalinin, B. J. Rodriguez, S. Jesse, E. Karapetian, B. Mirman, E. A. Eliseev, and A. N. Morozovska, Annu. Rev. Mater. Res. **37**, 189–238 (2007).
[10]T. Watanabe, H. Funakubo, and K. Saito, J. Mater. Res. **16**(1), 303–307 (2001).
[11]J. Schwarzkopf, R. Dirsyte, M. Rossberg, G. Wagner, and R. Fornari, Mater. Sci. Eng. B **144**, 132–137 (2007).
[12]T. Watanabe and H. Funakubo, Jpn. J. Appl. Phys., Part 1 **39**, 5211–5216 (2000).
[13]C. C. B. J. Rodriguez, S. V. Kalinin, and R. Proksch, Nanotechnology **18**(47), 475504 (2007).
[14]M. A. Zurbuchen, J. Lettieri, S. J. Fulk, Y. Jia, A. H. Carim, D. G. Schlom, and S. K. Streiffer, Appl. Phys. Lett. **82**(26), 4711–4713 (2003).
[15]S. Y. Yang, F. Zavaliche, L. Mohaddes-Ardabili, V. Vaithyanathan, D. G. Schlom, Y. J. Lee, Y. H. Chu, M. P. Cruz, Q. Zhan, T. Zhao, and R. Ramesh, Appl. Phys. Lett. **87**, 102903 (2005).
[16]C. D. Theis, J. Yeh, D. G. Schlom, M. E. Hawley, G. W. Brown, J. C. Jiang, and X. Q. Pan, Appl. Phys. Lett. **72**(22), 2817–2819 (1998).
[17]M. d. Keijser and G. J. M. Dormans, MRS Bull. **21**, 37 (1996).
[18]B. D. Cullity, *Elements of X-Ray Diffraction* (Addison-Wesley Publishing Company, Inc., 1956).
[19]X. Q. Pan, J. C. Jiang, C. D. Theis, and D. G. Schlom, Appl. Phys. Lett. **83**(12), 2315–2317 (2003).
[20]M. A. Zurbuchen, W. Tian, X. Q. Pan, D. Fong, S. K. Streiffer, M. E. Hawley, J. Lettieri, Y. Jia, G. Asayama, S. J. Fulk, D. J. Comstock, S. Knapp, A. H. Carim, and D. G. Schlom, J. Mater. Res. **22**(6), 1439–1471 (2007).